Acta Pharmaceutica Sinica B 2011;1(4):240–247

Institute of Materia Medica, Chinese Academy of Medical Sciences
Chinese Pharmaceutical Association

Acta Pharmaceutica Sinica B

www.elsevier.com/locate/apsb
www.sciencedirect.com

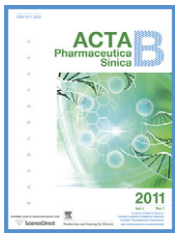

ORIGINAL ARTICLE

Design, synthesis and biological evaluation of novel histone deacetylase inhibitors based on virtual screening

Hui Lu, Ya-dong Chen, Bo Yang, Qi-dong You*

Department of Medicinal Chemistry, China Pharmaceutical University, Nanjing 210009, China

Received 20 September 2011; revised 9 October 2011; accepted 13 October 2011

KEY WORDS

Histone deacetylases;
Virtual screening;
Non-hydroxamate;
MS-275

Abstract Ligand- and structure-based virtual screening methods were employed to identify novel non-hydroxamate histone deacetylase (HDAC) inhibitors. Based on the newly identified hit compound **17a**, three series of compounds were synthesized and evaluated for both HDAC1 inhibitory activity and cytotoxicity. Binding modes of representative structures were analyzed using the docking method to explain the observed disparity in HDAC1 inhibitory activities.

*Corresponding author. Tel./fax: +86 25 83271351.
E-mail address: youqidong@gmail.com (Qi-dong You).

Peer review under responsibility of Institute of Materia Medica, Chinese Academy of Medical Sciences and Chinese Pharmaceutical Association.
doi:10.1016/j.apsb.2011.10.002

Production and hosting by Elsevier

1. Introduction

Histone deacetylases (HDACs) have been widely recognized as promising targets for cancer treatment. The primary activity of HDACs is to remove acetyl groups from the ε-amino groups of lysine residues in the N-terminal extension of the core histones, which results in chromatin condensation and transcriptional repression[1]. Eighteen mammalian HDACs have been identified and categorized into four structural and functionally distinct classes[2]. Class I (HDAC1–3 and 8), class II (HDAC4–7, 9 and 10) and class IV (HDAC11) HDACs share conserved residues in the catalytic core regions and require zinc ion for deacetylation, while class III (SIRT1–7) HDACs are unrelated sirtuin deacetylases and require NAD^+ for their enzymatic activity[3].

A vast number of HDAC inhibitors are currently under development and four representative structures are shown in Fig. 1. Vorinostat (SAHA) and romidepsin (FK228) have been approved by US FDA for the treatment of relapsed cutaneous T-cell lymphoma (CTCL)[4], and there are at least fourteen HDAC inhibitors under more than eighty clinical trials[5]. Most of the HDAC inhibitors have three common features: cap group, zinc binding group (ZBG) and hydrophobic spacer[6]. The hydroxamic acid moiety has been widely used as zinc binding group. Although it has strong metal chelating capability, it displays little isoform selectivity among class I, II and IV HDACs and might result in the inhibition of other metallo-enzymes or sequestration of metal ions. Hydroxamic acids also suffer from metabolic and pharmacokinetic problems such as rapid glucoronidation and sulfation[7].

Different types of non-hydroxamate functionalities have been reported, such as benzamides[8], electrophilic ketones[9], ketoamides[10], phosphonates[11], *N*-formylhydroxylamine[12] and so on. The 2-aminobenzamide derivative MS-275 presents excellent HDAC inhibitory activity and has been in phase I/II clinical trials for various solid tumors and hematological malignancies[8,13]. Nevertheless, many of the non-hydroxamate HDAC inhibitors have either reduced potency or metabolic disadvantages. Thus, there remains a need to develop HDAC inhibitors with new non-hydroxamate zinc binding group.

2. Results and discussion

2.1. Molecular design

X-ray crystal structures of human HDAC8[3,14,15] and two bacterial HDAC-like enzymes, namely HDLP from *Aquifex aeolicus* (related to class I HDACs)[16] and HDAH from *Bordetella/Alcaligenes* strain FB188 (related to class IIb HDACs)[17,18] have been resolved in 2000 s. HDAC8, which shares the same active site and zinc binding residues with HDAC1–3, was used in our virtual screening. The sequence homology between HDAC8 and HDAC1 is high with 31% sequence identity and 53% sequence similarity[19]. In 2010, a crystal structure of HDAC2 complexed with a benzamide inhibitor was solved[20]. HDAC2, which demonstrates 85.2% sequence identity with HDAC1, was used as the template for HDAC1 homology modeling to explicate the biological results.

We searched the database of NCI2000 (with 238,819 molecules) and MiniMaybridge (with about 2000 molecules) by pharmacophore-based virtual screening. Based on the crystal structure of HDAC8/TSA complex (PDB code: 1T64), the pharmacophore model was built manually by mapping the chemical features on the corresponding functional groups of TSA in its binding conformation (Fig. 2) using Catalyst as reported in the literature[21]. Particular spatial shape was generated based on the binding conformation of TSA using Catalyst default settings, which merged with pharmacophore features to form the query model for the first round virtual screening. 847 molecules were selected for the next round of screening.

Molecular docking program DOCK5.0 was employed for subsequent screening based on the crystal structure of HDAC8 (PDB code: 1T64). The protocol was verified by docking TSA back into HDAC8. The RMSD between the docking pose and the binding conformation in the crystal structure is 0.91 Å. The small molecules obtained were ranked according to their scores calculated by the energy scoring function in DOCK program. The top 300 molecules with best scores were subjected to drug-likeness analysis. Thirty compounds were finally chosen as candidate molecules for further investigation.

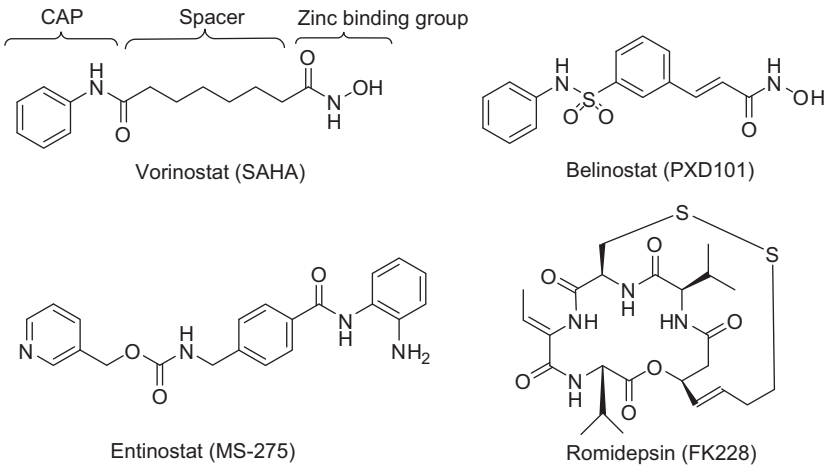

Figure 1 Examples of clinically tested HDAC inhibitors.

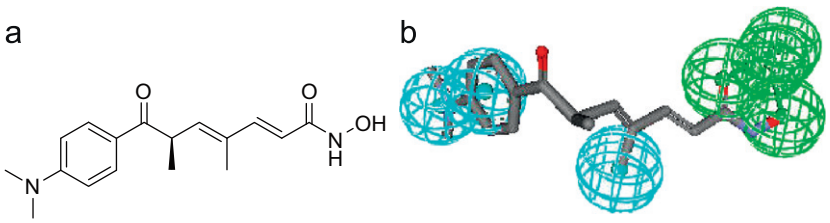

Figure 2 (a) Structure of Trichostatin A (TSA), a natural histone deacetylase inhibitor and (b) the pharmacophore model based on the bound conformation of TSA. The location constraints (dots and arrows) represent the ideal relative positions in space for the chemical functions, and the tolerance spheres (colored spheres) represent relative areas around the location constraints where chemical functions can still participate in mapping to the pharmacophore.

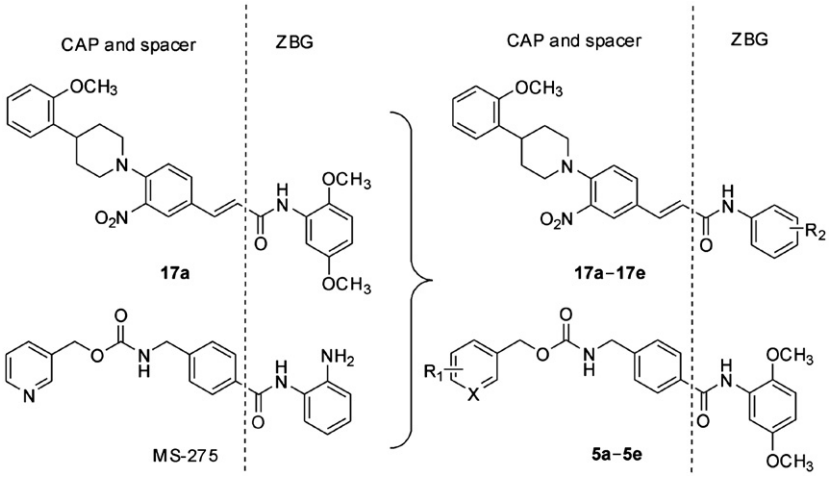

Figure 3 Design of new HDAC inhibitors by combining the structural features of **17a** and MS-275.

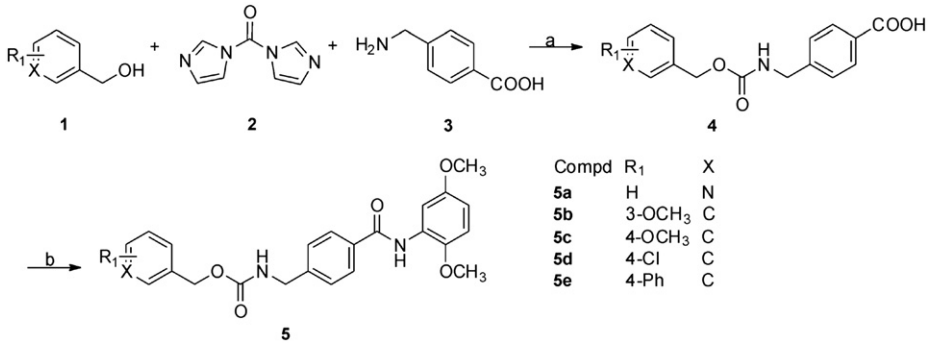

Scheme 1 Synthesis route of compounds **5a–e**. Reagents and conditions: (a) ① THF, 10 °C to rt; ② Et_3N, DBU, THF, rt, 50–60%; (b) 2,5-Dimethoxyaniline, PyBOP, Et_3N, DCM, 30–40%.

Among the 30 candidate molecules, compound **17a**, which is featured by its unique structure, was identified as a new hit compound with weak HDAC1 inhibitory activity. Compounds **5a–e** were designed by combining the cap group and spacer of MS-275 derivatives with the zinc binding group of **17a** to validate the potential of 2,5-dimethoxybenzamide as zinc binding group. While compounds **13a** and **13b** were designed by integrating the spacer and zinc binding group of MS-275 with cap group from **17a** to examine the feasibility of 4-(2-methoxyphenyl)piperidine as a new cap group. Compounds **17b-e** were derivatives of **17a** with various substituted benzamides to explore the effects of different substitutions on the inhibitory activity against HDACs (as shown in Fig. 3).

2.2. *Chemistry*

The general approach to synthesize compounds **5a–e** is outlined in Scheme 1. Condensation of 3-(hydroxymethyl)pyridine or substituted phenyl methanol (**1**) with 4-(aminomethyl)benzoic acid (**3**) using 1,1′-carbonyldiimidazole (**2**) gave carboxylic acids **4**, which underwent an amide coupling reaction with 2,5-dimethoxyaniline to afford **5**.

The synthetic route of compounds **13a–b** is outlined in Scheme 2. Grignard Reaction of *tert*-butyl-4-oxopiperidine-1-carboxylate (**6**) and 1-bromo-2-methoxybenzene (**7**), followed by dehydration and deprotection in 6 N HCl and reduction under 50 psi, gave 4-(2-methoxyphenyl)piperidine hydrochloride (**10**).

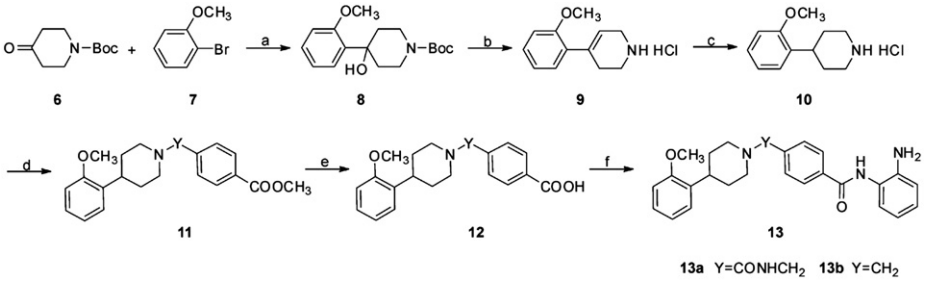

Scheme 2 Synthesis route of compounds **13a** and **13b**. Reagents and conditions: (a) Mg, I_2, dry THF, N_2 protected, 40 °C to reflux, 56%; (b) 6N HCl, reflux, 63%; (c) 10% Pd/C, H_2, CH_3OH, 50 psi, 78%; (d) Methyl 4-(aminomethyl)benzoate, Et_3N, triphosgene, DCM (for **11a** 47%); or methyl 4-formylbenzoate, $NaBH_4$, CH_3OH, reflux (for **11b** 63%); (e) 1 mol/L LiOH, THF, rt, 87% and (f) 1, 2-Phenylenediamine, BOP, Et_3N, DMF, rt, 30%.

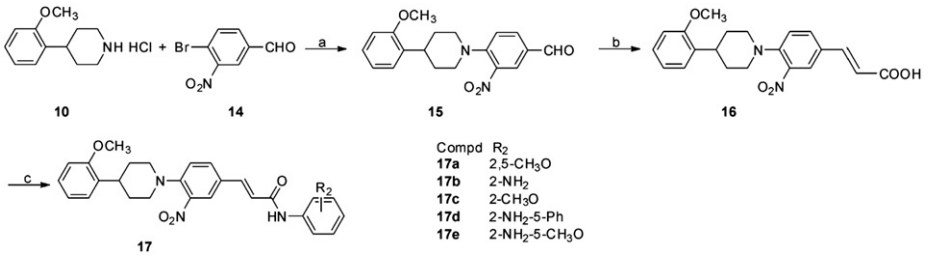

Scheme 3 Synthesis route of compounds **17a-e**. Reagents and conditions: (a) Et_3N, tol/DMF (5:1), reflux, 69%; (b) Malonic acid, piperidine, pyridine, reflux, 78%; (c) Substituted aniline, PyBOP, Et_3N, DCM, rt (for **17a** 32%, **17b** 47% and **17c** 56%); or (1) Substituted aniline, PyBOP, Et_3N, DCM, rt; (2) TFA/DCM; (3) 10% NaOH (for **17d** 23% and **17e** 31%).

Treatment of **10** and methyl 4-(aminomethyl)benzoate with triphosgene gave urea **11a**. Reductive amination of **10** with methyl 4-formylbenzoate and $NaBH_4$ provided **11b**. The intermediates **11** were hydrolyzed and condensed with 1,2-phenylenediamine to afford amides **13**.

The synthesis of compounds **17a–e** is presented in Scheme 3. Nucleophilic aromatic substitution of 4-bromo-3-nitrobenzaldehyde (**14**) with **10**, followed by Knoevenagel Reaction produced intermediate **16**. In the last steps, condensation of **16** with different substituted anilines and successive deprotection led to **17**.

2.3. *Biological evaluation*

2.3.1. *HDAC1 enzyme inhibition assay*

Binding modes of benzamide HDAC inhibitors have been demonstrated in HDAC2/benzamides complex. The hydrogen atoms of the *ortho*-NH_2 group are involved in hydrogen bonds with the side chains of histidines 145 and 146, the nitrogen of the *ortho*-NH_2 group chelates the zinc, and the carbonyl oxygen interacts with both the tyrosine side chain hydroxyl and the zinc.

Compounds **5a–e** are MS-275 derivatives with 2-aminobenzamide replaced by 2,5-dimethoxybenzamide from **17a**. Compounds **5a–e** were evaluated using an HDAC1 enzyme inhibition assay and the results were shown in Table 1. As the oxygen atom is more electronegative than the nitrogen atom, it might result in weaker coordination with the zinc ion, and this fact might explain the observation that none of these compounds showed significant HDAC1 inhibitory activities. The results also implicates that a potent zinc binding group is crucial for HDAC inhibitory activity.

Compounds **13a** and **13b** are MS-275 derivatives with 4-(2-methoxyphenyl)piperidine as the cap group. The percentage inhibition of both compounds is slightly higher than that of MS-275 (Table 2), which suggests favorable interactions of 4-(2-methoxyphenyl)piperidine with the enzyme.

We further examined **17a** derivatives with different substituted benzamides (Table 3) to investigate the effects of different substitutions on the inhibition of HDACs. Compound **17b** with 2′-aminobenzamide showed noticeable HDAC1 inhibitory activity (35.99% inhibition at the concentration of 50 μmol/L). Replacing the 2′-aminobenzamide (**17b**) with 2-methoxybenzamide (**17c**) resulted in decreased inhibitory activity, which is consistent with the above result that the oxygen atom of methoxyl group might have weaker affinity with the zinc ion. Introduction of 5′-phenyl substituent on the aniline ring (**17d**) increased the potency remarkably, while incorporation of 5′-methoxyl substituent (**17e**) had no effects on potency. These results supported the recognition that the phenyl moiety may be optimal for binding in the narrow entry to the internal cavity of the zinc active site, while methoxyl group is probably too bulky to fit the internal cavity[22–24].

2.3.2. *Molecular docking*

To obtain information on the structural basis of the observed disparity in HDAC1 inhibitory activities, we docked three 2′-aminobenzamide containing compounds MS-275, **13a** and **17a** into HDAC1 homology model using a validated molecular dock program (GOLD)[25,26]. The homology model was constructed as described in the literature[19]. Independent docking of MS-275 (89.64% inhibition), **13a** (95.36% inhibition) and **17a** (35.99% inhibition) revealed that these compounds exhibited preferences for different binding modes at the pocket rim (as shown in Fig. 4). For MS-275 and **13a**, pyridine and 4-(2-methoxyphenyl)piperidine interact with Tyr 195 at the

Table 1 Biological activities of MS-275 derivatives **5a–e** containing 2,5-dimethoxybenzamide as potential zinc binding group.

Compound	R_1	X	Clog P	% Inhibition of HDAC1 at 50 μmol/L	Cytotoxicity (IC_{50}, μmol/L)		
					HCT-116	MCF-7	HUVEC
17a	–	–	5.048	25.76±0.82	>50	>50	>50
5a	H	N	1.559	21.07±1.23	19.43	23.56	>50
5b	3-OCH_3	C	2.975	25.63±2.42	35.13	15.11	12.42
5c	4-OCH_3	C	2.975	ND[a]	14.67	31.22	>50
5d	4-Cl	C	3.769	10.92±0.98	>50	ND[a]	>50
5e	4-Ph	C	4.944	16.20±12.27	16.83	30.56	>50
MS-275	–	–	0.822	89.64±2.84	1.32	23.76	>50

ND[a]: not determined.

Table 2 Biological activities of MS-275 derivatives **13a** and **13b** with 4-(2-methoxyphenyl)piperidine as cap group.

Compound	Y	Clog P	% Inhibition of HDAC1 at 50 μmol/L	Cytotoxicity (IC_{50}, μmol/L)		
				HCT-116	MCF-7	HUVEC
17a	–	5.048	25.76±0.82	>50	>50	>50
13a	$CONHCH_2$	2.677	95.36±1.62	1.26	19.0	15.6
13b	CH_2	3.377	93.98±0.33	2.12	18.1	34.7
MS-275	–	0.822	89.64±2.84	1.32	23.76	>50

Table 3 Biological activities of **17a** derivatives with different substituted benzamides as zinc binding groups.

Compound	R_2	Clog P	% Inhibition of HDAC1 at 50 μmol/L	Cytotoxicity (IC_{50}, μmol/L)		
				HCT-116	MCF-7	HUVEC
17a	2, 5-CH_3O	5.048	25.76±0.82	>50	>50	>50
17b	2-NH_2	4.311	35.99±2.29	2.48	>50	>50
17c	2-CH_3O	5.023	25.76±2.63	>50	>50	>50
17d	2-NH_2-5-Ph	6.199	47.79±0.76	>50	>50	>50
17e	2-NH_2-5-CH_3O	4.447	30.92±0.20	4.94	>50	>50
MS-275	–	0.822	89.64±2.84	1.32	23.76	>50

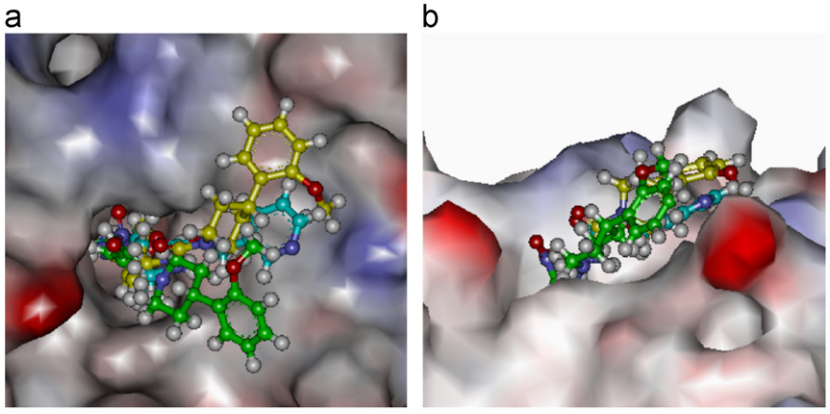

Figure 4 GOLD docking solutions for MS-275 (blue), **13a** (yellow) and **17a** (green) at HDAC1; (a) Up view of the surface of HDAC1 near the active site and (b) Side view of the benzamides–HDAC1 interaction.

rim of the binding pocket. For the binding mode of **17a**, the structure at the entrance of the active site is not flexible enough to enable the interaction between 4-(2-methoxyphenyl)piperidine and Tyr 195. This docking result explains the low potency of compounds **17**, and suggests that interaction between the cap group and the enzyme surface is crucial for HDAC inhibitory activity and the rigidity of the spacer could affect potency by defining the orientation of the cap group.

2.3.3. *Cytotoxic activity in vitro*

All compounds were evaluated for cytotoxicity to human colon cancer HCT-116 cells, human breast adenocarcinoma MCF-7 cells and human umbilical vein endothelial cells (HUVEC) using the 3-(4,5-dimethylthiazol-2-yl)-2,5-diphenyl tetrazolium bromide (MTT) assay. As shown in Table 1, compounds **5a–e** showed modest cytotoxicity to HCT-116 and MCF-7 cells in concert with their low HDAC1 inhibitory activities. Compounds **13a** and **13b** exhibited excellent anti-proliferative activity to HCT-116 cells. Nevertheless, they also showed cytotoxicity to HUVEC (Table 2). As shown in Table 3, compounds **17a** and **17e** exhibited similar anti-proliferative activity against HCT-116 cells with MS-275 and have no cytotoxicity to HUVEC. Though **17d** presented the highest potency against HDAC1 in compounds **17**, it showed no anti-proliferative activity to HCT-116 cells. ClogP values were calculated using Chemdraw. Compounds **17a**, **17c** and **17d** which showed no anti-proliferative activity to HCT-116 cells all have CLogP values greater than 5.

3. Conclusions

In summary, ligand- and structure-based virtual screening was employed to identify novel non-hydroxamate HDAC inhibitors. Based on the newly identified hit compound **17a**, three series of compounds were synthesized and evaluated on both HDAC1 inhibitory activity and cytotoxicity. Binding modes of representative structures were analyzed using the docking method. MS-275 derivatives **5a–e** with 2,5-dimethoxybenzamide as zinc binding group showed weak HDAC1 inhibitory activities suggesting methoxyl as a poor zinc binding group. Replacement of pyridine in MS-275 with 4-(2-methoxyphenyl)piperidine increased the potency. Compounds **13a** and **13b** presented HDAC1 inhibitory activities and anti-proliferative activity to HCT-116 cells, but they also showed cytotoxicity to HUVEC. **17a** derivatives exhibited modest HDAC1 inhibitory activities, which according to the docking analysis was due to the lack of flexibility precluding the interaction of the cap group with enzyme surface. Our work provided some insights to the binding interactions of inhibitors with HDAC and could facilitate development of novel non-hydroxamate HDAC inhibitors.

4. Experimental

4.1. *Chemical synthesis*

Melting points were determined on Thomas Hoover apparatus. Infrared spectra were acquired on Nicolet Impact 410 spectrophotometer using a KBr film. The absorption band is given in cm^{-1}. ^1H NMR spectra were recorded on a Bruker ACF-300 spectrometer (300 MHz). Chemical shifts are presented in ppm relative to tetramethylsilane. Mass spectra were obtained on a Mariner Mass Spectrum, or a GC-2010 mass spectrometer. Elemental analyses were determined on a Carlo Erba 1106 elementary analysis apparatus.

4.2. *General procedures to prepare amides*

Method A: A mixture of benzoic acid (1 eq.), PyBOP (1 eq.) and triethylamine (1.2 eq.) in dichloromethane was stirred at room temperature for 15 min. Substituted phenylamine (1.2 eq.) was then added. The mixture was stirred at room temperature for 8 h. The solvent was removed under reduced pressure, and the crude product so-obtained was purified by column chromatography.

Method B: A mixture of benzoic acid (1 eq.), BOP (1.2 eq.) and triethylamine (1.2 eq.) in *N*,*N*-dimethylformamide (DMF) was stirred at room temperature for 10 min. Substituted phenylamine (1.2 eq.) was then added. The mixture was stirred at room temperature overnight. Aqueous sat. NH_4Cl (15 mL) was added to the mixture and the crude product was collected by filtration and purified by column chromatography.

4.2.1. *N-[[4-[[(2,5-dimethoxyphenyl)amino]carbonyl] phenyl]methyl]-3-pyridinylmethyl ester (**5a**)*

^1H NMR (DMSO-d_6) δ: 3.72 (3H, s), 3.80 (3H, s), 4.29 (2H, d, J=6.3 Hz), 5.11 (2H, s), 6.73 (1H, dd, J=9.0 Hz, J=3.0 Hz), 7.01(1H, d, J=9.0 Hz), 7.38–7.44 (3H, m), 7.56 (1H, d, J=3.0 Hz), 7.80 (1H, d, J=7.8 Hz), 7.91 (1H, d, J=8.1 Hz), 7.99 (1H, t, J=6.0 Hz), 8.54 (1H, d, J=4.2 Hz), 8.61 (1H, s), 9.31 (1H, s). MS (ESI) m/z: 422.1 $[M+H]^+$. IR (KBr) cm^{-1}: 3382, 3225, 1721, 1528, 1274, 1043. *Anal.* Calcd for $C_{23}H_{23}N_3O_5$: C, 66.55; H, 5.50; N, 9.97. Found: C, 66.13; H, 5.98; N, 9.65.

4.2.2. *N-[[4-[[(2,5-dimethoxyphenyl)amino]carbonyl] phenyl]methyl]-3-methoxyphenylmethyl ester (**5b**)*

^1H NMR (DMSO-d_6) δ: 3.72 (3H, s), 3.75 (3H, s), 3.80 (s, 3H), 4.29 (2H, d, J=6.3 Hz), 5.04 (2H, s), 6.73 (1H, dd, J=9.0 Hz, J=3.0 Hz), 6.94–6.90 (3H, m), 7.01(1H, d, J=9.0 Hz), 7.26–7.32 (1H, m), 7.30 (2H, d, J=8.1 Hz), 7.56 (1H, d, J=3.0 Hz), 7.89–7.97 (3H, m), 9.31 (1H, s). MS (ESI) m/z: 451.1 $[M+H]^+$. IR (KBr) cm^{-1}: 3318, 1687, 1650, 1536, 1273, 1057. *Anal.* Calcd for $C_{25}H_{26}N_2O_6$: C, 66.65; H, 5.82; N, 6.22. Found: C, 66.46; H, 5.73; N, 6.21.

4.2.3. *N-[[4-[[(2,5-dimethoxyphenyl)amino]carbonyl] phenyl]methyl]-4-methoxyphenylmethyl ester (**5c**)*

^1H NMR (DMSO-d_6) δ: 3.72 (3H, s), 3.75 (3H, s), 3.80 (3H, s), 4.27 (2H, d, J=9.0 Hz), 4.98 (2H, s), 6.73 (1H, dd, J=9.0 Hz, J=3.0 Hz), 6.93 (2H, d, J=8.4 Hz), 7.01 (1H, d, J=9.0 Hz), 7.31 (2H, d, J=8.4 Hz), 7.38 (2H, d, J=9.0 Hz), 7.55 (1H, d, J=3.0 Hz), 7.83–7.97 (3H, m), 9.30 (1H, s). MS (ESI) m/z: 451.1 $[M+H]^+$. IR (KBr) cm^{-1}: 3345, 2940, 1712, 1650, 1536, 1251. *Anal.* Calcd for $C_{25}H_{26}N_2O_6$: C, 66.65; H, 5.82; N, 6.22. Found: C, 66.60; H, 6.10; N, 6.14.

4.2.4. *4-chlorobenzyl 4-(2,5-dimethoxyphenylcarbamoyl) benzylcarbamate (**5d**)*

^1H NMR (DMSO-d_6) δ: 3.72 (3H, s), 3.80 (3H, s), 4.28 (2H, d, J=5.7 Hz), 5.10 (2H, s), 6.71–6.74 (1H, m), 7.01 (1H, d,

J=9.0 Hz), 7.38–7.56 (6H, m), 7.89–7.99 (3H, m), 9.30 (1H, s). MS (ESI) m/z: 455.4 $[M+H]^+$. IR (KBr) cm^{-1}: 3340, 1512, 1465, 1300, 1247. *Anal*. Calcd for $C_{24}H_{23}ClN_2O_5^{\bullet}$ 3/2 H_2O: C, 659.81; H, 5.44; N, 5.81. Found: C, 59.55; H, 5.76; N, 5.72.

4.2.5. *N-[[4-[[(2,5-dimethoxyphenyl)amino]carbonyl] phenyl]methyl]-4-biphenylmethyl ester* (**5e**)

^1H NMR (DMSO-d_6) δ: 3.68 (3H, s), 3.72 (3H, s), 4.29 (2H, d, J=6.3 Hz), 5.11 (2H, s), 6.72 (1H, dd, J=9.0 Hz, J=3.0 Hz), 7.01 (1H, d, J=9.0 Hz), 7.34–7.49 (6H, m), 7.55 (1H, d, J=3.0 Hz), 7.67 (4H, d, J=7.5 Hz), 7.89–7.56 (3H, m), 9.30 (1H, s). MS (ESI) m/z: 497.2 $[M+H]^+$. IR (KBr) cm^{-1}: 3353, 1693, 1530, 1261, 1225, 1046. *Anal*. Calcd for $C_{30}H_{28}N_2O_5$: C, 72.56; H, 5.68; N, 5.64. Found: C, 72.31; H, 5.93; N, 5.63.

4.2.6. *N-(4-(2-aminophenylcarbamoyl)benzyl)-4-(2-methoxyphenyl)piperidine-1-carboxamide* (**13a**)

^1H NMR (DMSO-d_6) δ: 1.26–1.68 (2H, m), 1.81–1.85 (2H, m), 2.88–2.97 (2H, m), 3.08–3.16 (1H, m), 3.83 (3H, s), 4.08–4.12 (2H, m), 4.47–4.48 (2H, m), 6.85–6.96 (4H, m), 7.08–7.22 (3H, m), 7.32–7.39 (3H, m), 7.83 (2H, d, J=7.8 Hz), 8.13(1H, s). MS (ESI) m/z: 457.1 $[M+H]^+$. IR (KBr) cm^{-1}: 3287, 2921, 1622, 1550, 1241, 752. *Anal*. Calcd for $C_{27}H_{30}N_4O_3$: C, 70.72; H, 6.59; N, 12.22. Found: C, 70.82; H, 6.37; N, 12.07.

4.2.7. *N-(2-aminophenyl)-4-((4-(2-methoxyphenyl) piperidin-1-yl)methyl)benzamide* (**13b**)

^1H NMR (DMSO-d_6) δ: 1.83–1.92 (4H, m), 3.14 (3H, m), 3.44–3.47 (2H, m), 3.80 (3H, s), 4.42 (2H, br s), 6.60–6.65 (1H, m), 6.80 (1H, d, J=7.8 Hz), 6.92–7.00 (3H, m), 7.12–7.26 (3H, m), 7.66 (2H, d, J=7.5 Hz), 8.1 (2H, d, J=7.5 Hz). MS (EI) m/z: 415 (M^+). IR (KBr) cm^{-1}: 3385, 3020, 1652, 1504, 1455, 1236, 845. *Anal*. Calcd for $C_{26}H_{29}N_3O_2$: C, 75.15; H, 7.03; N, 10.11. Found: C, 75.23; H, 7.28; N, 9.87.

4.2.8. *(E)-N-(2,5-dimethoxyphenyl)-3-(4-(4-(2-methoxyphenyl)piperidin-1-yl)-3-nitrophenyl)acrylamide* (**17a**)

^1H NMR (DMSO-d_6) δ: 1.53–1.87 (4H, m), 2.98–3.11 (3H, m), 3.36–3.40 (2H, m), 3.74 (3H, s), 3.77 (3H, s), 3.81 (3H, s), 6.43 (1H, d, J=15.3 Hz), 6.53 (1H, dd, J=9.0 Hz, J=3.0 Hz), 6.75 (1H, d, J=9.0 Hz), 6.81 (1H, d, J=8.1 Hz), 6.87 (1H, m), 7.06 (1H, d, J=8.7 Hz), 7.16 (2H, d, J=7.5 Hz), 7.52 (1H, dd, J=8.7 Hz, J=2.1 Hz), 7.58 (1H, d, J=15.3 Hz), 7.90 (1H, s), 7.94 (1H, d, J=2.1 Hz), 8.19 (1H, d, J=2.7 Hz). IR (KBr) cm^{-1}: 2955, 2833, 1679, 1650, 1530, 1208, 1019. MS (ESI) m/z: 518.3 $[M+H]^+$. *Anal*. Calcd for $C_{29}H_{31}N_3O_6$: C, 67.30; H, 6.04; N, 8.12. Found: C, 67.01; H, 6.02; N, 8.43.

4.2.9. *(E)-N-(2-aminophenyl)-3-(4-(4-(2-methoxyphenyl) piperidin-1-yl)-3-nitrophenyl)acrylamide* (**17b**)

^1H NMR ($CDCl_3$) δ: 1.90 (4H, m), 3.04–3.20 (3H, m), 3.41–3.46 (2H, m), 3.84 (3H, s), 6.52 (1H, d, J=15.3 Hz), 6.79–6.84 (2H, m), 6.90–6.93 (1H, m), 6.95–6.98 (1H, m), 7.05–7.12 (2H, m), 7.18–7.24 (2H, m), 7.28–7.31 (1H, m), 7.53–7.66 (3H, m), 7.96 (1H, s). IR (KBr) cm^{-1}: 3413, 3365, 1664, 1605, 1525, 1384, 1218. MS (ESI) m/z: 473.2 $[M+H]^+$. *Anal*. Calcd for $C_{27}H_{28}N_4O_4$: C, 68.63; H, 5.97; N, 11.86. Found: C, 68.72; H, 5.94; N, 12.09.

4.2.10. *(E)-N-(2-methoxyphenyl)-3-(4-(4-(2-methoxyphenyl)piperidin-1-yl)-3-nitrophenyl)acrylamide* (**17c**)

^1H NMR (DMSO-d_6) δ: 1.88–1.93 (4H, m), 3.05–3.16 (3H, m), 3.43–3.47 (2H, m), 3.84 (3H, s), 3.93 (3H, s), 6.51 (1H, d, J=15.6 Hz), 6.87–7.14 (6H, m), 7.18–7.26 (2H, m), 7.57–7.68 (2H, m), 7.95–8.02 (2H, m), 8.50 (1H, d, J=7.4 Hz). IR (KBr) cm^{-1}: 3347, 1676, 1608, 1529, 1458. MS (ESI) m/z: 488.2 $[M+H]^+$. *Anal*. Calcd for $C_{28}H_{29}N_3O_5$: C, 68.98; H, 6.00; N, 8.62. Found: C, 69.02; H, 6.02; N, 8.57.

4.2.11. *(E)-N-(4-aminobiphenyl-3-yl)-3-(4-(4-(2-methoxyphenyl)piperidin-1-yl)-3-nitrophenyl)acrylamide* (**17d**)

^1H NMR (DMSO-d_6) δ: 1.87–1.88 (4H, m), 3.00–3.14 (3H, m), 3.36–3.40 (2H, m), 3.83 (3H, s), 6.51 (1H, d, J=15.6 Hz), 6.82–7.02 (4H, m), 7.18–7.37 (6H, m), 7.42–7.62 (5H, m), 7.89–7.94 (2H, m). IR (KBr) cm^{-1}: 3377, 1608, 1526, 1490, 1237. MS (ESI) m/z: 549.4 $[M+H]^+$. *Anal*. Calcd for $C_{33}H_{32}N_4O_4$: C, 72.24; H, 5.88; N, 10.21. Found: C, 72.24; H, 6.00; N, 10.23.

4.2.12. *(E)-N-(2-amino-5-methoxyphenyl)-3-(4-(4-(2-methoxyphenyl)piperidin-1-yl)-3-nitrophenyl)acrylamide* (**17e**)

^1H NMR (DMSO-d_6) δ: 1.83 (4H, m), 2.98–3.14 (3H, m), 3.35–3.39 (2H, m), 3.67 (3H, s), 3.77 (3H, s), 6.44 (1H, d, J=15.3 Hz), 6.56–6.59 (1H, m), 6.73 (1H, d, J=8.7 Hz), 6.81 (1H d, J=8.1 Hz), 6.88 (1H, t, J=7.5 Hz), 7.04 (1H d, J=8.7 Hz), 7.12–7.19 (3H, m), 7.25 (1H, m), 7.49 (1H, d, J=7.8 Hz), 7.58 (1H, d, J=15.6 Hz), 7.74 (1H, s), 7.90 (1H, s). IR (KBr) cm^{-1}: 2955, 2833, 1679, 1650, 1530, 1208, 1019. MS (ESI) m/z: 503.2 $[M+H]^+$. *Anal*. Calcd for $C_{28}H_{30}N_4O_5$: C, 66.92; H, 6.02; N, 11.15. Found: C, 66.47; H, 5.89; N, 11.43.

4.3. *Biological evaluation*

4.3.1. *Fluorimetric HDAC1 assay*

The HDAC1 fluorescent activity assay was based on the Fluor de Lys Substrate and Developer combination (BioMol), carried out according to the supplier's instructions. First, the Fluor de Lys Substrate, which comprises an acetylated lysine side chain, was incubated with purified recombinant HDAC1 enzymes in the presence or the absence of test compounds. Deacetylation of the substrate sensitizes the substrate so that, in the second step, treatment with the Developer produces a fluorophore. Fluorescence was quantified with a TECAN inphinite M200 station.

4.3.2. *In vitro cytotoxicity assay*

All compounds were dissolved in DMSO at a stock concentration of 10 mg/mL, and diluted with fresh medium before assays. Cell lines were seeded into 96-well flat bottom plates at density of 6000 cells/well. Twelve hours after seeding, each compound dilution was added in duplicate and incubation continued at 37 °C in a humidified atmosphere containing 5% CO_2. After 72 h, 20 μL MTT at 5 mg/mL in PBS (filter sterilized, light protected, and stored at 4 °C) was added to each well, and after 4 h of incubation at 37 °C, the fluorescence was measured at 570 nm using Thermo Multiskan Spectrum.

References

1. Bolden JE, Peart MJ, Johnstone RW. Anticancer activities of histone deacetylase inhibitors. *Nat Rev Drug Discov* 2006;**5**:769–84.
2. Gregoretti IV, Lee YM, Goodson HV. Molecular evolution of the histone deacetylase family: functional implications of phylogenetic analysis. *J Mol Biol* 2004;**338**:17–31.
3. Vannini A, Volpari C, Gallinari P. Substrate binding to histone deacetylases as shown by the crystal structure of the HDAC8–substrate complex. *EMBO Rep* 2007;**8**:879–84.
4. Zain J, Kaminetzky D, O'Connor OA. Emerging role of epigenetic therapies in cutaneous T-cell lymphomas. *Expert Rev Hematol* 2010;**3**:187–203.
5. Tan J, Cang S, Ma Y, Petrillo RL, Liu D. Novel histone deacetylase inhibitors in clinical trials as anti-cancer agents. *J Hematol Oncol* 2010. doi:10.1186/1756-8722-3-5.
6. Paris M, Porcelloni M, Binaschi M, Fattori D. Histone deacetylase inhibitors: from bench to clinic. *J Med Chem* 2008;**51**:1505–29.
7. Mulder GJ, Meerman JH. Sulfation and glucuronidation as competing pathways in the metabolism of hydroxamic acids: the role of N,O-sulfonation in chemical carcinogenesis of aromatic amines. *Environ Health Perspect* 1983;**49**:27–32.
8. Suzuki T, Ando T, Tsuchiya K. Synthesis and histone deacetylase inhibitory activity of new benzamide derivatives. *J Med Chem* 1999;**42**:3001–3.
9. Vasudevan A, Ji Z, Frey RR. Heterocyclic ketones as inhibitors of histone deacetylase. *Bioorg Med Chem Lett* 2003;**13**:3909–13.
10. Wada CK, Frey RR, Ji Z. Alpha-keto amides as inhibitors of histone deacetylase. *Bioorg Med Chem Lett* 2003;**13**:3331–5.
11. Kapustin GV, Fejer G, Gronlund JL, McCafferty DG, Seto E, Etzkorn FA. Phosphorus-based SAHA analogues as histone deacetylase inhibitors. *Org Lett* 2003;**5**:3053–6.
12. Wu TY, Hassig C, Wu Y, Ding S, Schultz PG. Design, synthesis, and activity of HDAC inhibitors with a N-formyl hydroxylamine head group. *Bioorg Med Chem Lett* 2004;**14**:449–53.
13. Gore L, Rothenberg ML, O'Bryant CL. A phase I and pharmacokinetic study of the oral histone deacetylase inhibitor, MS-275, in patients with refractory solid tumors and lymphomas. *Clin Cancer Res* 2008;**14**:4517–25.
14. Somoza JR, Skene RJ, Katz BA. Structural snapshots of human HDAC8 provide insights into the class I histone deacetylases. *Structure* 2004;**12**:1325–34.
15. Vannini A, Volpari C, Filocamo G. Crystal structure of a eukaryotic zinc-dependent histone deacetylase, human HDAC8, complexed with a hydroxamic acid inhibitor. *Proc Natl Acad Sci USA* 2004;**101**:15064–9.
16. Finnin MS, Donigian JR, Cohen A. Structures of a histone deacetylase homologue bound to the TSA and SAHA inhibitors. *Nature* 1999;**401**:188–93.
17. Nielsen TK, Hildmann C, Dickmanns A, Schwienhorst A, Ficner R. Crystal structure of a bacterial class 2 histone deacetylase homologue. *J Mol Biol* 2005;**354**:107–20.
18. Nielsen TK, Hildmann C, Riester D, Wegener D, Schwienhorst A, Ficner R. Complex structure of a bacterial class 2 histone deacetylase homologue with a trifluoromethylketone inhibitor. *Acta Crystallogr Sect F: Struct Biol Cryst Commun* 2007;**63**:270–3.
19. Wang DF, Helquist P, Wiech NL, Wiest O. Toward selective histone deacetylase inhibitor design: homology modeling, docking studies, and molecular dynamics simulations of human class I histone deacetylases. *J Med Chem* 2005;**48**:6936–47.
20. Bressi JC, Jennings AJ, Skene R. Exploration of the HDAC2 foot pocket: synthesis and SAR of substituted *N*-(2-aminophenyl)benzamides. *Bioorg Med Chem Lett* 2010;**20**:3142–5.
21. Chen Y, Li H, Tang W. 3D-QSAR studies of HDACs inhibitors using pharmacophore-based alignment. *Eur J Med Chem* 2009; **44**:2868–76.
22. Vaisburg A, Paquin I, Bernstein N. *N*-(2-amino-phenyl)-4-(heteroarylmethyl)-benzamides as new histone deacetylase inhibitors. *Bioorg Med Chem Lett* 2007;**17**:6729–33.
23. Witter DJ, Harrington P, Wilson KJ. Optimization of biaryl selective HDAC1&2 inhibitors (SHI-1:2). *Bioorg Med Chem Lett* 2008;**18**:726–31.
24. Methot JL, Chakravarty PK, Chenard M. Exploration of the internal cavity of histone deacetylase (HDAC) with selective HDAC1/HDAC2 inhibitors (SHI-1:2). *Bioorg Med Chem Lett* 2008;**18**:973–8.
25. Thangapandian S, John S, Sakkiah S, Lee KW. Ligand and structure based pharmacophore modeling to facilitate novel histone deacetylase 8 inhibitor design. *Eur J Med Chem* 2010;**45**:4409–17.
26. Schafer S, Saunders L, Eliseeva E. Phenylalanine-containing hydroxamic acids as selective inhibitors of class IIb histone deacetylases (HDACs). *Bioorg Med Chem* 2008;**16**:2011–33.